



Mapping critical cortical hubs and white matter pathways by direct electrical stimulation: an original functional atlas of the human brain

Silvio Sarubbo^{a,*,1}, Matthew Tate^{b,1}, Alessandro De Benedictis^c, Stefano Merler^d,
Sylvie Moritz-Gasser^{e,f}, Guillaume Herbet^{e,f}, Hugues Duffau^{e,f}

^a Division of Neurosurgery, Structural and Functional Connectivity Lab Project, Azienda Provinciale per i Servizi Sanitari (APSS), 9 Largo Medaglie d'Oro, 38122, Trento, Italy

^b Departments of Neurosurgery and Neurology, Northwestern University, Feinberg School of Medicine, 420 E Superior St, 60611, Chicago, IL, USA

^c Neurosurgery Unit, Department of Neuroscience and Neurorehabilitation, Bambino Gesù Children's Hospital IRCCS, 4 Piazza Sant'Onofrio, 00165, Rome, Italy

^d Bruno Kessler Foundation (FBK), Trento, Italy

^e Department of Neurosurgery, Gui de Chauliac Hospital, Montpellier University Medical Center, 80 Avenue Augustin Fliche, Montpellier, France

^f National Institute for Health and Medical Research (INSERM), U1051, Team "Plasticity of the Central Nervous System, Human Stem Cells and Glial Tumors", Institute for Neurosciences of Montpellier, Montpellier University Medical Center, 80 Av Augustin Fliche, Montpellier, France

ARTICLE INFO

Keywords:

Atlas
Brain functions
Brain mapping
Direct electrical stimulation
White matter
Subcortical

ABSTRACT

Objective: The structural and functional organization of brain networks subserving basic daily activities (i.e. language, visuo-spatial cognition, movement, semantics, etc.) are not completely understood to date. Here, we report the first probabilistic cortical and subcortical atlas of critical structures mediating human brain functions based on direct electrical stimulation (DES), a well-validated tool for the exploration of cerebral processing and for performing safe surgical interventions in eloquent areas.

Methods: We collected 1162 cortical and 659 subcortical DES responses during testing of 16 functional domains in 256 patients undergoing awake surgery. Spatial coordinates for each functional response were calculated, and probability distributions for the entire patient cohort were mapped onto a standardized three-dimensional brain template using a multinomial statistical analysis. In addition, matching analyses were performed against prior established anatomy-based cortical and white matter (WM) atlases.

Results: The probabilistic maps for each functional domain were provided. The topographical analysis demonstrated a wide spatial distribution of cortical functional responses, while subcortical responses were more restricted, localizing to known WM pathways. These DES-derived data showed reliable matching with existing cortical and WM atlases as well as recent neuroimaging and neurophysiological data.

Conclusions: We present the first integrated and comprehensive cortical-subcortical atlas of structures essential for humans' neural functions based on highly-specific DES mapping during real-time neuropsychological testing. This novel atlas can serve as a complementary tool for neuroscientists, along with data obtained from other modalities, to improve and refine our understanding of the functional anatomy of critical brain networks.

1. Introduction

Since the origin of the medical sciences, the brain has been considered the most complex human organ and the core of human intelligence (Crivellato and Ribatti, 2007; Hutchison et al., 2013). Over the last three decades, the exploration of brain structures and functional processing experienced substantial advances, most notably due to non-invasive

neuroimaging techniques such as functional MRI (fMRI) and diffusion-weighted imaging (DWI) tractography. Task-based and resting-state fMRI provided insights into the functional organization and plasticity of brain networks, while DWI offered visualization of white matter (WM) pathways underlying network connectivity, opening the era of the brain connectome (Sporns, 2013). The integration of fMRI, lesion maps (Fox, 2018), and tractography provided notable contributions to

* Corresponding author. Division of Neurosurgery, Structural and Functional Connectivity Lab Project, "S. Chiara" Hospital, Azienda Provinciale per i Servizi Sanitari (APSS), 9, Largo Medaglie d'Oro, 38122, Trento, Italy.

E-mail address: silviosarubbo@gmail.com (S. Sarubbo).

¹ These authors contributed equally.

<https://doi.org/10.1016/j.neuroimage.2019.116237>

Received 22 May 2019; Received in revised form 25 September 2019; Accepted 30 September 2019

Available online 15 October 2019

1053-8119/© 2019 Elsevier Inc. This is an open access article under the CC BY-NC-ND license (<http://creativecommons.org/licenses/by-nc-nd/4.0/>).

the definition of network circuitry underlying brain processing (Petersen and Sporns, 2015) and a large volume of original data. Despite their obvious importance in neuroscience research, fMRI and DTI do have some limitations (van den Heuvel et al., 2017; Maier-Hein et al., 2017; Pujol et al., 2015). For instance, while fMRI may delineate which brain areas involved in a given function, it does not indicate which of these regions are critical, and DTI, despite its interest and widespread adoption into neuroscience over the last decade, does not provide functional information about human WM pathways. Thus, there is a critical need for simple, direct, and reproducible measurements of brain function that can serve as a starting point for a more sophisticated understanding of human brain network organization and function.

In this context, the application of cortical-subcortical direct electrical stimulation (DES) during resection of low-grade gliomas (LGGs), allowed reliable, original and reproducible evidence for the functional assessment of different brain networks (Duffau, 2015; Thiebaut de Schotten et al., 2005; Rech et al., 2014; Sarubbo, 2016; Herbet et al., 2014). Moreover, despite the fact that LGGs infiltrate cortical and subcortical WM sites, this method has demonstrated added contributions relative to other brain mapping techniques [i.e. electro-encephalography, cortico-cortical evoked-potentials, transcranial magnetic stimulation (EEG, CCEPs, TMS)] (Matsumoto et al., 2004, 2012; Michel and Murray, 2012). In particular, DES is currently considered the primary technique in neurosurgical practice for the identification of critical network components at both the cortical and the subcortical levels, allowing neurosurgeons to preserve neurologic functions despite resections in or near eloquent areas (Sanai et al., 2008; Sanai and Berger, 2010; Duffau et al., 2005a). It is worth noting that DES is not the only technique that provides information about the putative properties of the cortices, but it does constitute the unique method to investigate the functional role also of WM connections during mapping. Thus DES has allowed the computation of cortical and subcortical probabilistic functional atlases of the human brain that are consistent with the current neuroscience literature (Ius et al., 2011; Tate et al., 2014; Sarubbo et al., 2015a; Herbet et al., 2016). However, no studies are available integrating cortical and subcortical DES data for a given function, nor validating such findings using independent non-DES data sets.

Here, we propose, for the first time to our knowledge, an integrated probabilistic atlas of the critical hubs and connections subserving fundamental human brain functions, based on a series of 1821 functional responses collected by DES in 256 patients undergoing awake craniotomy. We defined these maps according to a comprehensive and practical description of the cortical and subcortical brain regions required for key domains of human brain processing, as determined by DES during real-time neuropsychological evaluation. For each individual functional response evoked during DES, we provide MNI coordinates, with the goal of proposing a practical and complementary atlas for supporting, refining, validating, and driving brain network analyses.

2. Material and methods

2.1. Patient characteristics and intraoperative mapping paradigm

256 patients [mean age: 38.7 years] with WHO grade II LGGs were included (demographics and general information are reported in Table 1). An asleep-awake-asleep protocol was utilized, with sedation stopped just prior to the awake mapping portion of the surgery (Tate et al., 2014; Sarubbo et al., 2015a; Sarubbo, 2016). DES was performed to identify essential cortical epicenters and subcortical pathways, according to the technique previously reported (Herbet et al., 2014; Duffau et al., 2005a; Tate et al., 2014; Sarubbo et al., 2015a; Hau et al., 2017). Briefly, a bipolar electrode with 5 mm spacing was used to deliver a biphasic current to the brain surface or subcortical white matter (60 Hz; 2–4 mA; 1 msec pulse duration). During awake mapping, the DES intensity threshold was determined by either evoking speech arrest (without facial or tongue movements) during a counting task (from 0 to 10) within the

Table 1
Patients demographics.

Patients (N°)	256
Age at surgery (years)	38.7 ± 10.3
Male/Female	135/121
Tumor location (%)	
Left	60.6
Right	39.4
Handedness (%)	
Right	85.1
Left	9.4
Ambidextrous	5.5
Tumor Distribution	%
Frontal	69
Temporal	56
Frontal-temporal-insular	40
Frontal-insular	32
Parietal	23
Temporal-insular	18
Temporal-parietal	8
Insular	2
Frontal-parietal	2
Temporal-occipital	2

ventral pre-motor cortex (VPMC) or by evoking motor (i.e. muscle contraction) and/or sensory (i.e. dysesthesias) responses during stimulation of the primary motor or sensory areas [the pre-central (Pre-CG) or post-central gyrus (Post-CG), respectively]. This threshold was used for the remainder of the mapping session. The entire exposed cortical surface was electrically interrogated, even beyond the borders of the lesion, to define a map of functionally critical brain regions (Fig. 1). During the tumor resection, patients were asked to continuously perform specific tasks that were designed according to the cortical and subcortical pathways that the neurosurgeon was expected to encounter during resection (rather than all 16 tasks at each cortical/subcortical site, which would have been impractical given intraoperative time limitations). For the purposes of this study, subcortical mapping referred to the WM bundles and/or caudate/basal ganglia that was exposed at the depth of the surgical resection cavity. The entire area of subcortical WM exposed during the resection was mapped using the same current threshold identified during the initial cortical mapping (Fig. 1). With respect to DES-defined mapping sites, a “positive” functional site referred to a cortical/subcortical region that either promoted a functional response (in the case of motor and sensory mapping) or altered normal behavior (in the case of all other functional categories tested). Specific examples of positive functional mapping sites are detailed below in the “Neuropsychological Testing” section.

When all functional limits of the resection were reached (i.e. the boundaries of the surgical cavities resulted in eloquent responses with DES at both the cortical and subcortical levels), the resection was stopped. Functional responses were marked with numerical tags, and intra-operative digital images of the cortical and subcortical DES-defined maps were stored for offline analyses, specifically direct comparison with the pre- and post-operative anatomic MRI.

2.2. Neuropsychological testing

Motor functions were monitored in two ways: (1) overt muscle twitch noted during cortical or subcortical stimulation and (2) alteration of a continuous complex motor task (simultaneous hand, arm and forearm flexion-extension contralateral to the lesion side) during stimulation, specifically acceleration, deceleration, or halting of movement. Sensory responses were reported verbally by the patient during cortical and subcortical mapping, in particularly dysesthesias of the contralateral face, arm, or leg during stimulation (Duffau et al., 2005a, 2008). Spontaneous language production was monitored by a counting paradigm (series from 0 to 10) and repetition test, with positive functional

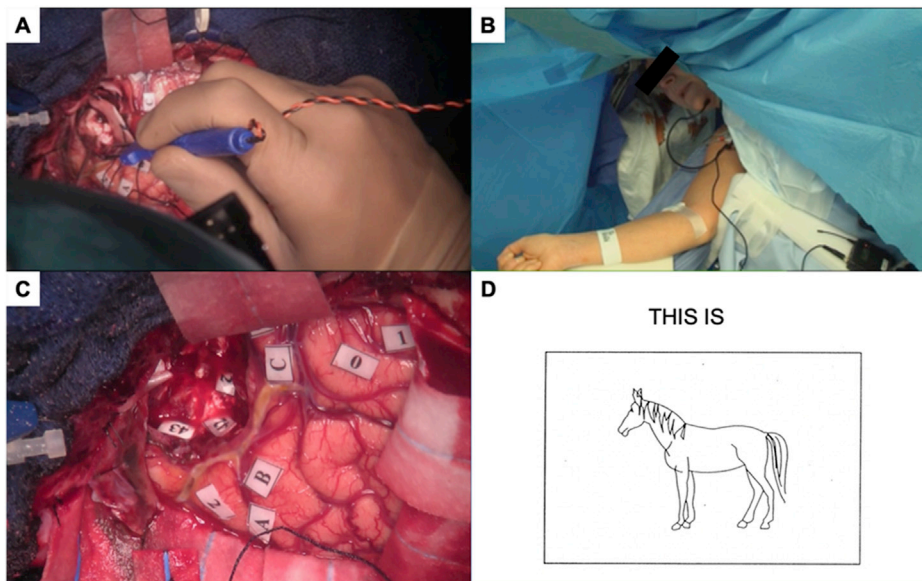


Fig. 1. Intra-operative direct electrical stimulation-based mapping. In panel A, the surgeon is stimulating the subcortical white matter of the middle temporal gyrus using a standard hand-held bipolar stimulator while the patient (panel B) is performing a classical naming task. Panel C shows the final cortical (tags 0,1,2,A,B,C) and subcortical (42,43) positive mapping sites. For the naming task, the patient is asked to name the object presented on a computer screen (D) while the neurosurgeon stimulates sites at the cortical and subcortical white matter. In this case, the correct response is “This is a horse.” If the patient makes an error during stimulation at a particular site, the type of error is noted, such as anomia (patient says “This is a ...”) but cannot come up with “horse”), semantic paraphasias (e.g. patient incorrectly says “This is a cow.” instead of “This is a horse.”), phonemic paraphasias (e.g. patient incorrectly says “This is a hearse.” instead of “This is a horse.”), speech arrest (no verbal output), or verbal perseveration (patient correctly says “This is a horse” but when a different object is shown after a delay, the patient incorrectly states “This is a horse.” again). In the example depicted in this figure, stimulation of the white matter region corresponding to site 42 (Panel C) caused an anomia. The MNI coordinates (x,y,z) corresponding to site 42 is derived by normalizing this patient’s brain to MNI space and manually plotting this subcortical point onto the normalized brain. For the group mapping and matching analyses, this point is combined with normalized coordinates of all other anomia sites from the entire cohort of subjects.

responses being involuntary cessation of counting or inability to repeat, respectively, during stimulation (Coello et al., 2013; Mandonnet et al., 2017). Phonologic and semantic aspects of language processing (i.e. semantic and phonological paraphasias or pure anomia, not related to motor/praxis/visual disturbances) and reading (i.e. alexia or reading disturbances) were assessed with picture naming [denomination object 80 (DO 80)] and reading tests, respectively, as previously reported (Duffau et al., 2003, 2005a, 2008; Mandonnet et al., 2017; Deloche et al., 1991). Examples of positive functional responses included semantic paraphasias (e.g. patient says “dog” instead of cat during presentation of a picture of a cat), phonemic paraphasias (e.g. patient says “kite” instead of cat after presentation of a picture of a cat), and anomias (e.g. patient states “this is a ...”) but cannot come up with “cat” during presentation of a cat picture). Such patient errors during stimulation were monitored by a speech therapist (S.M.-G.) or by a neuropsychologist (G.H.). Non-verbal semantic disorders (namely, asemantism) were identified with the pyramid-palm-tree test (PPTT). For the PPTT, a picture is shown and the patient asked to select the one picture (from a choice of two) that goes with the original picture (Moritz-Gasser et al., 2013; Herbert et al., 2015). Visual field, visual functions and eye movements were monitored, as previously described (Montemurro et al., 2016; Gras-Combe et al., 2012; Sarubbo et al., 2015b). Spatial cognition was assessed with a line bisection task, according to the technique previously described, where the patient is presented with a standard length line and asked to mark the midpoint with a pen (Thiebaut de Schotten et al., 2005; Bartolomeo et al., 2007). Functional responses related to mentalizing (i.e. understanding, and consequently predicting, mental and psychological states and behaviors) were assessed using a variant of the classical Reading the Mind in the Eyes Test (Herbet et al., 2015), in which the patient is presented with a set of eyes and then asked to choose (from a list of four) the emotional state. Importantly, during these tasks, both the patient and neuropsychologist/speech therapist were blinded to the timing of DES performed by the surgeon.

2.3. Atlas computation

All patients underwent volumetric T1-weighted MRI with gadolinium 3 months after surgery. These sequences were normalized spatially to the Montreal Neurologic Institute (MNI) 152 template brain space, at 1 mm³ voxel spatial resolution (Evans et al., 1992). Non-brain structures were removed from the T1-images with the brain extraction tool (BET) of the FMRIB software library (FSL; <http://www.fmrib.ox.ac.uk/fsl>). Registration of resulting images was performed by applying 12 parameter affine transformations using FSL’s linear image registration tool (FLIRT). Of note, this method proved more reliable than non-linear registration methods that were explored due to factors specific to patients harboring brain tumors (brain shift, local mass effect, sizeable resection cavity, ventricular changes). As previously described (Herbet et al., 2014; Tate et al., 2014; Sarubbo et al., 2015a, Sarubbo, 2016), the MNI coordinates of the functional subcortical and cortical responses, collected during intra-operative DES, were extracted by the first and second authors (S.S. and M.T.), two expert anatomists with previous experiences in these atlas methods. Each stimulation point was manually plotted onto a digitized asymmetric human brain template (MNI ICBM152, 1-mm resolution) using a combination of regional cortical (sulci, vessels) and subcortical (resection cavity) landmarks, T1-weighted MRI reconstructed on three planes (axial, sagittal and coronal), and dictated operative reports. Three-dimensional coordinates (x, y, z) in MNI space were recorded and reported for each cortical and subcortical point for subsequent group-level analyses.

2.4. Probabilistic distribution of cortical and subcortical functional responses

The MNI location *x* corresponds to an individual DES-induced functional response for a given function *R* (e.g. semantic, motor, etc.) in a single patient. The null hypothesis tested in our methodology was that no

functional response was present at a given cortical or subcortical site (rather than a different functional response). As previously detailed (Sarubbo et al., 2015a), based on the diameter of the bipolar DES electrode (5 mm), we assume that all voxels y of the brain in MNI space at a distance ≤ 0.5 cm from x have the same functional response R . Also, similar to the aforementioned analysis (Herbet et al., 2014; Tate et al., 2014; Sarubbo et al., 2015a, Sarubbo, 2016), let R_1, \dots, R_k be the set of k functional responses considered in this study (e.g. semantic, motor, etc.), and let x be a voxel of the brain in MNI space. We assume that any voxel x is associated with a vector $\pi(x) = (\pi_1(x), \dots, \pi_k(x))$, where $\pi_i(x)$ is the probability that voxel x is involved in the processing of the functional response R_i . Let us assume that $n(x)$ functional response errors have been induced by DES at voxel x in our patient series, obtaining $l_i(x)$ functional response errors of type R_i , with $\sum_{i=1}^k l_i(x) = n(x)$. We assume that the number of outcomes $l_i(x)$ follows a multinomial distribution with parameters $n(x)$ and $\pi(x)$. Therefore, the probability function of this multinomial distribution is: $f(l_1(x), \dots, l_k(x); n(x), \pi(x)) = \frac{n(x)!}{l_1(x)! \dots l_k(x)!} \pi_1^{l_1(x)}(x) \dots \pi_k^{l_k(x)}(x)$. The maximum likelihood estimate of any individual probability $\pi_i(x)$ is $p_i(x) = l_i(x)/n(x)$. Maximum likelihood estimates $p_i(x)$, derived by varying x in the MNI space, represent statistical maps in the MNI space of the probability that voxels x are involved in the processing of functional responses R_i . As a check of validity of the proposed method, statistical maps $p_i(x)$ consistently match with those previously reported (Tate et al., 2014; Sarubbo et al., 2015a).

2.5. Matching analysis

In order to provide a quantitative analysis of the data, for comparison with recent literature, and to validate our stimulation point localization technique, we performed a partition of our brain model into 176 cortical and cortical plus white matter anatomical ROIs, according to the extensively adopted JHU Atlas (Zhang et al., 2010). For each spatial map $p_i(x)$, we computed the percentage of the maps of the functional responses overlapping the ROIs of this anatomic atlas.

Finally, we computed the distance of any subcortical functional response from all the WM pathways of the tractography atlas of Nat-BrainLab (available at: <http://www.natbrainlab.co.uk/atlas-maps>) (Thiebaut de Schotten et al., 2011a). The distance of a stimulus from a given bundle of the atlas was defined as the minimal Euclidean distance between the stimulus and the set of voxels defining the tract itself, as previously described (Sarubbo et al., 2015a). This allowed us to quantify the distribution of the distance of the different functional responses R_i from the main bundles of the human WM, as reconstructed in the most recent version of this established tool.

3. Results

An overall number of 1821 positive responses (1162 cortical, 659 subcortical) were collected by using DES among 16 functional domains.

The total number of cortical functional responses collected included: reading (2), anomia (94), asomatognosia [i.e. comprehension disorders during execution of PPTT (17)], eye movement control (4), mentalizing (12), motor (325), motor control (89), phonological (14), semantic (39), somatosensory (150), spatial perception (23), speech output (251), speech articulation (142). Subcortical functional responses included: acoustic (2), reading (13), anomia (31), non-verbal comprehension (20), eye movement control (7), language and motor planning (24), mentalizing (14), motor (103), motor control (72), phonological (69), semantic (131), somatosensory (69), spatial perception (12), speech output (27), speech articulation (42), and visual (23).

The probabilistic distribution of the cortical and subcortical responses for each function among the entire patient cohort is reported in Figs. 2–4. Sagittal, coronal, and axial slices (spacing = 10 mm) along the respective MNI coordinates (x, y, z), illustrate the probability distribution, including

a color scale reflecting the confidence interval of each function, plotted onto the MNI 152 brain template and based on the multinomial statistical analysis.

For example, the first two panels of Fig. 2 report the distribution of motor and sensory responses, with the highest probability voxels, as expected, in the mid-portion of the pre- and post-central gyri, respectively.

The results of the matching analysis of the DES-defined functional responses with the major subcortical pathways as reconstructed in Nat-BrainLab Atlas are shown in the graphs of Fig. 5. Data are presented as the distance from subcortical DES points to the known WM pathways.

Finally, the overlap of DES-based data with the cortical and the cortical plus superficial WM ROIs of the JHU Atlas are reported in Tables 2 and 3.

4. Discussion

4.1. General considerations

Brain disorders represent an increasingly important problem for public health, given the high incidence and costs of diagnosis/treatment, as well as the increased level of physical and social disability, as the worldwide population ages. Accordingly, understanding the functional and structural organization of the human brain has been a key challenge not only for the neurosciences but also for the medical community. Recently, the National Institutes of Health in the United States established the Human Connectome Project (HCP), with the goal of mapping critical human brain structures and functions in healthy subjects over the lifespan. While the HCP has primarily focused on neuroimaging data in healthy subjects, multimodal research methods in both healthy and patient populations will be needed to develop reliable maps of human brain networks (Toga et al., 2006).

We computed a detailed three-dimensional probability distribution atlas for critical human brain functions with the largest stimulation-based functional dataset of the human brain to date (1187 functional responses in 256 patients). This “heat map” has, as an unprecedented feature, the capacity to integrate direct functional responses at both the cortical and the subcortical level obtained by stimulation. As a consequence, it may serve as a minimal and highly-specific anatomic-functional background for integration with different neuroimaging data as well as other functional (fMRI, TMS, EEG, etc.) and structural (i.e. tractography) datasets, with the goal of resolving the “true” governing principles behind physiologic brain processing, as well as patterns of re-organization following injury, i.e. neuroplasticity.

4.2. Functional considerations

4.2.1. Motor and somatosensory

The distribution of involuntary movements during DES reflects the classical cortical-subcortical distribution of the primary motor system, involving the pre-central gyrus (PreCG) and the corticospinal (CS) pathway (Fig. 2). (Duffau, 2015; Sarubbo et al., 2015a; Penfield and Boldrey, 1937) Sensory stimuli are distributed according to the classical cortical-subcortical organization of the somatosensory system, including the post-central gyrus (PostCG) and the thalamo-cortical pathways (Fig. 2). However, considering together these motor and sensory responses, our results suggest a non-rigid separation between the PreCG and the PostCG, as initially described by Penfield (Penfield and Boldrey, 1937). Rather, a strict reciprocal integration between the motor and sensory networks emerges, subserved by short inter-gyral WM connections (Catani et al., 2012). It is worth noting the high overlap of the cortical and subcortical responses with the Pre- and Post-CG ROIs of the JHU Atlas (Table 2) and the course of the tractography pathways (see also graphs in Fig. 5) confirms the reliable alignment of the data in the MNI space.

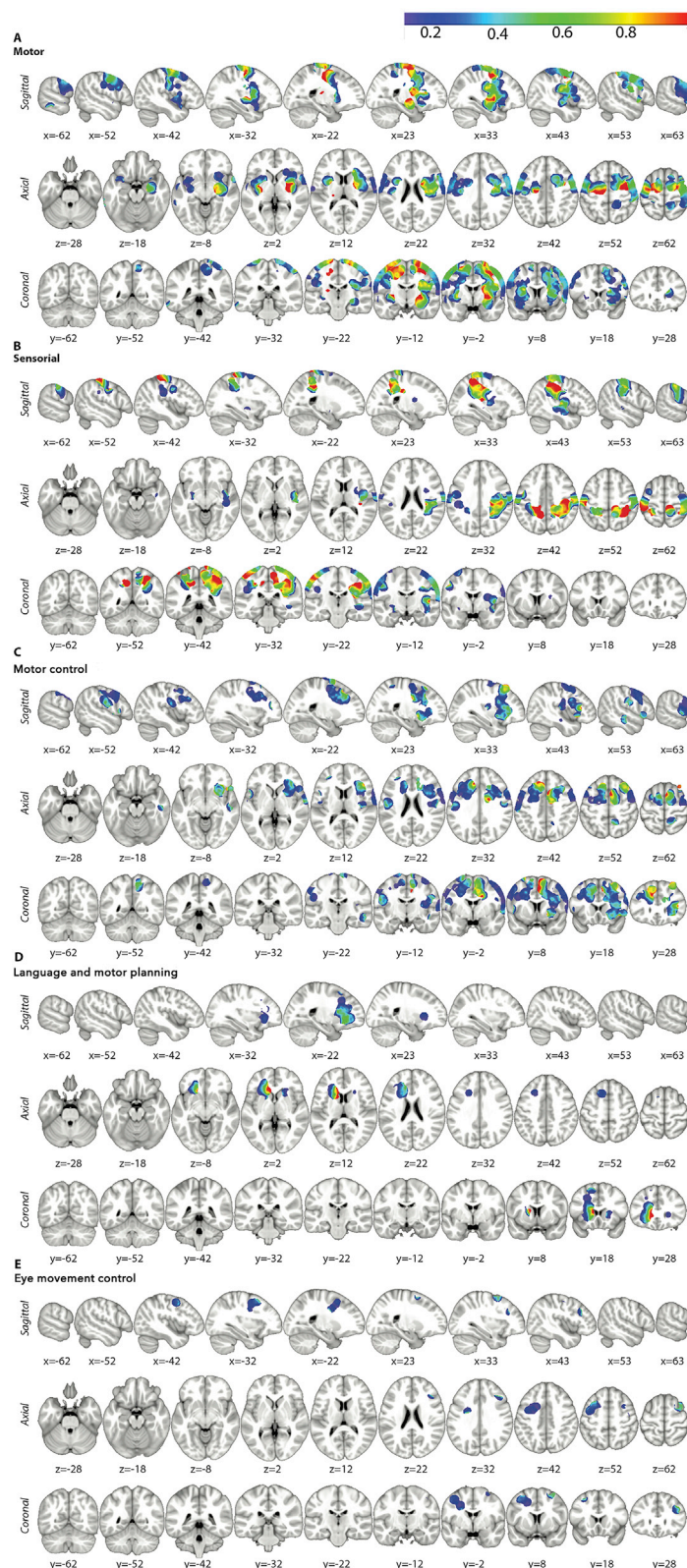


Fig. 2. The probability distribution along with confidence intervals mapped onto volumetric (1 mm) MNI T1 background (axial, sagittal, and coronal planes; 10 mm spacing) are demonstrated for the following functional responses: motor (A), sensory (B), motor control (C), language and motor planning (D), and eye movement control (E).

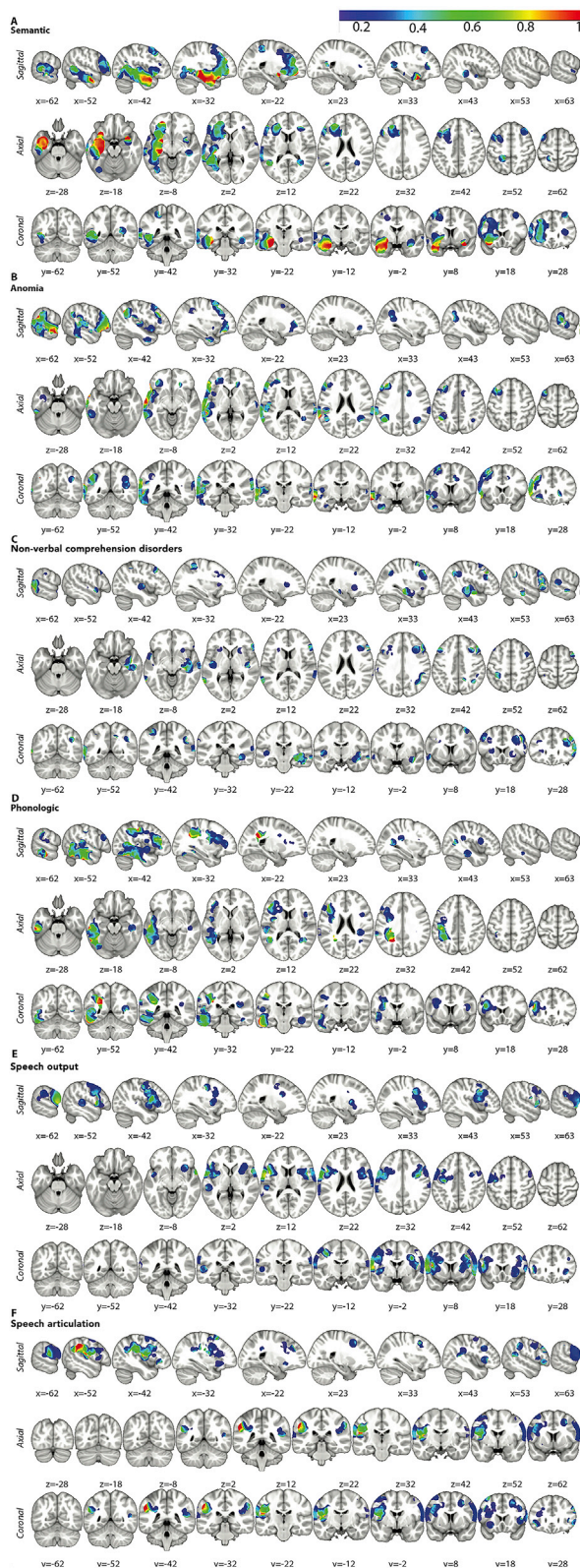


Fig. 3. The probability distribution, along with confidence intervals, mapped onto volumetric (1 mm) MNI T1 sequences (axial, sagittal and coronal planes; 10 mm spacing) are plotted for the following functional responses: semantic (A), anomia (B), non-verbal comprehension (C), phonologic (D), speech output (E), and speech articulation (F).

4.2.2. Motor control and language/motor planning

The distribution of the stimuli related to disorders of motor initiation and control, including movement arrest, confirms that awareness and control of voluntary movements depend on a network involving the dorsal-medial and lateral pre-motor cortices as well as the basal ganglia (Fig. 2). A complex framework of inhibitory and excitatory connections with a somatotopic organization characterizes this circuitry (Rech et al., 2016). In particular, the cortical distribution of stimuli related to interruption of the motor task confirms the key role of supplementary motor area (SMA), PreSMA, dorso-lateral pre-motor cortex (DLPFC), PreCS, insula and basal ganglia in the so-called “negative motor network” necessary for movement selection and pacing of voluntary movements (Duffau, 2015; Sarubbo et al., 2015a; Hoffstaedter et al., 2012; Schucht et al., 2013; Wolpe et al., 2014). A complex network of short and mid-range cortico-cortical and cortico-striatal fibers connects these regions, running in the deep WM of the frontal lobe (anteriorly to the pyramidal tract responsible for pure motor responses) (Catani et al., 2012; Schucht et al., 2013). Language and motor planning errors resulting in motor/verbal perseverations (Fig. 2) occurred predominantly during subcortical stimulation and mainly at the level of the caudate or neighboring WM. These results confirm the crucial role of the caudate in integrating the cortico-basal ganglia circuitry for the initiation, execution, and control of movements (Alexander and Crutcher, 1990).

4.2.3. Eye movement control

Disorders of eye movements have a cortical-subcortical distribution at the posterior part of the middle frontal gyrus (MFG) in both hemispheres (Fig. 2), which corresponds to the frontal eye fields. These results confirm the participation of this region in the network mediating motor initiation and control (Duffau, 2015) with a concordant topography with respect to the definition of the crucial region for control of eyes movement and integration in spatial working memory (Courtney et al., 1998).

4.2.4. Speech output

The representation of cortical and subcortical speech output response errors (speech arrest) is bilateral and symmetric, confirming a prevalent distribution within the most ventral portion of the pre-motor cortex and the underlying WM (Fig. 3). (Tate et al., 2014; Sarubbo et al., 2015a) The occurrence of complete speech arrest after stimulation of the ventral pre-motor cortex (VPMC), as previously reported, regardless of the side stimulated, suggests a possible bi-hemispheric integration of the articulatory loop network as previously proposed in a detailed stimulation study (Tate et al., 2014) and recently highlighted in a multimodal study integrating resting-state fMRI and DES (Zacà et al., 2018).

4.2.5. Speech articulation

The cortical and subcortical distribution of speech articulation errors (verbal apraxia) during stimulation in the ventral cortices of the PreCG, PostCG, supramarginal gyrus (SMG), and in the underlying WM (Fig. 3), including the indirect anterior component of superior longitudinal fascicle (SLF) (Catani et al., 2005), confirms the crucial role of the VPMC and this frontal-parietal network for converting the phonological information in articulatory motor output (Duffau et al., 2014). This characterization of the speech articulatory network is also concordant with analyses combining resting-state fMRI, DES, and tractography (Zacà et al., 2018) and with CCEPs studies in humans (Matsumoto et al., 2004).

4.2.6. Anomia

The high frequency of subcortical anomia at the junction below the posterior temporal cortices [middle and posterior thirds of STG and middle temporal gyrus (MTG)] and the inferior parietal lobule [particularly, the angular gyrus (AG)] (Fig. 3), matching the course of the indirect posterior component of the SLF, is likely a consequence of deactivation of visuo-semantic integration (Martino et al., 2013). In fact, the temporal-parietal-occipital junction represents a crucial region for visual-semantic processing and integration of this functional substrate

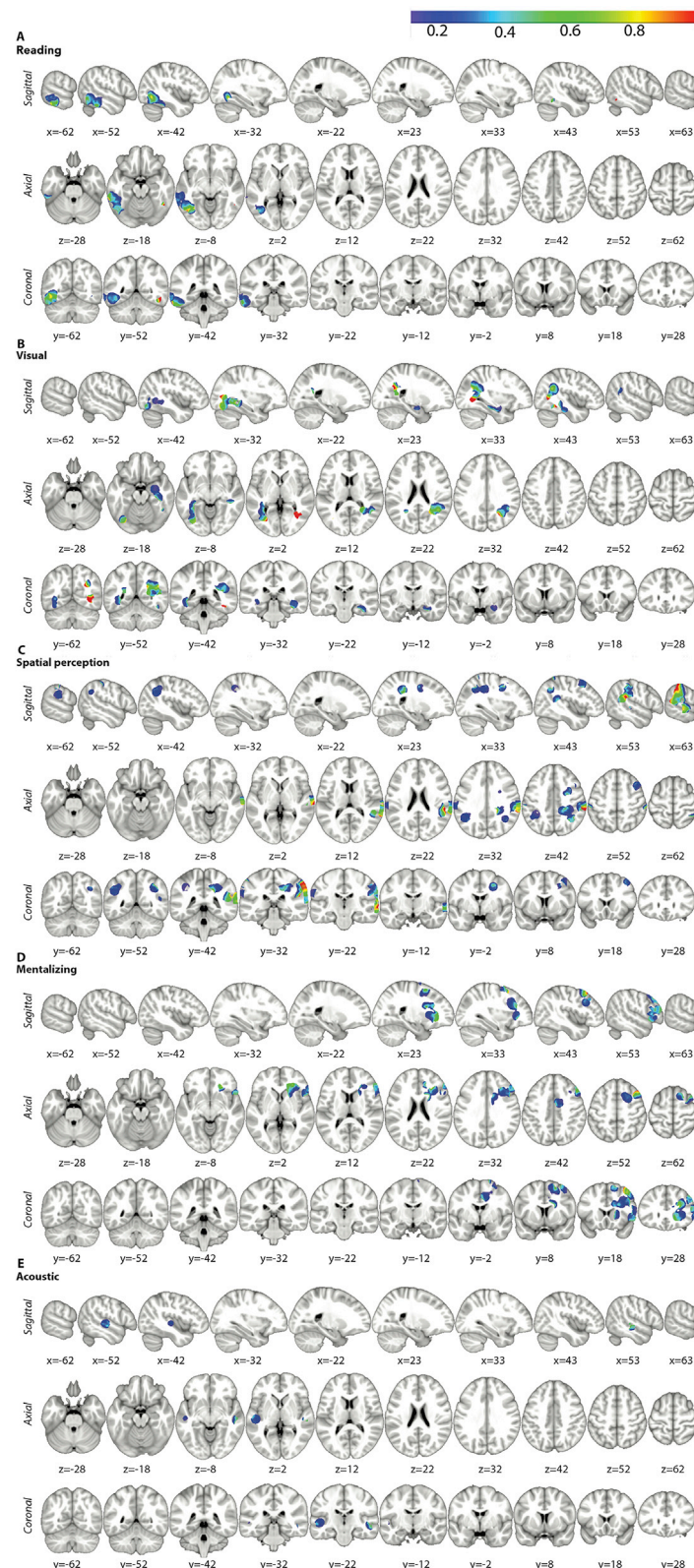


Fig. 4. The probability distribution, along with confidence intervals, mapped onto volumetric (1 mm) MNI T1 sequences (axial, sagittal and coronal planes; 10 mm spacing) are plotted for the following functional responses: reading (A), visual (B), spatial perception (C), mentalizing (D), and acoustic (E).

into the dorsal stream (Zemmoura et al., 2015; De Benedictis et al., 2014). From an anatomical point of view, this region includes an intersection of terminations of dorsal and ventral pathways [namely, indirect anterior and posterior SLF, arcuate fascicle (AF), inferior longitudinal fascicle (ILF), inferior fronto-occipital fascicle (IFOF)], as seen in the

dorso-ventral posterior frontal lobe [namely, inferior frontal gyrus (IFG) and DLPFC] where terminations of IFOF, indirect anterior SLF and uncinate fascicle (UF) are adjacent and may overlap (Sarubbo, 2016; Martino et al., 2013; De Benedictis et al., 2014).

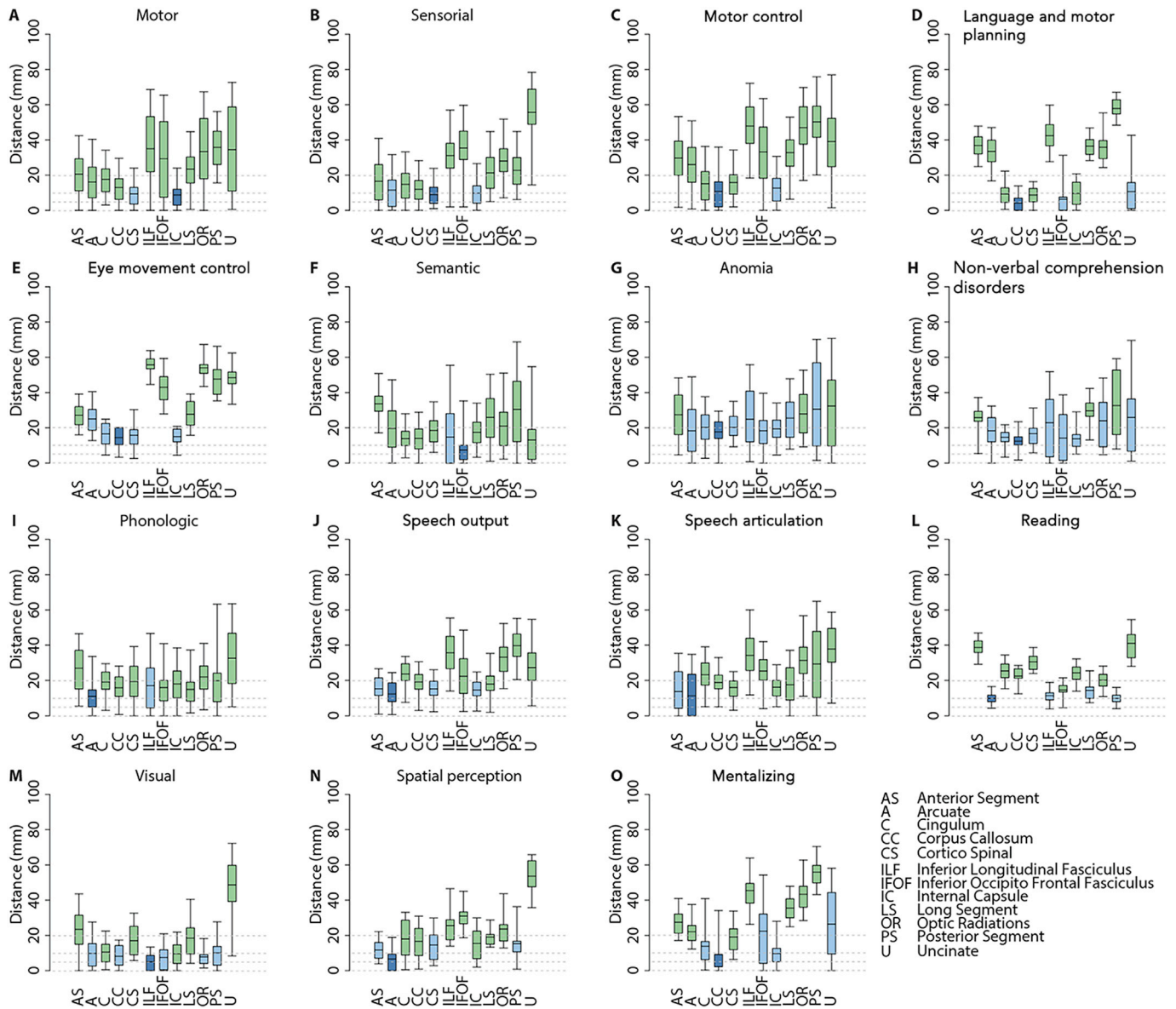


Fig. 5. In panels A–O we report the distributions (mean, 50% and 95% quantiles) of the distance of the different subcortical functional responses from the course of main white matter tracts, as reconstructed in the NatBrainLab Atlas (available at <http://www.natbrainlab.co.uk/atlas-maps>). In each panel the dark blue box plot represents the tract with minimal mean distance; the light blue box plots represent tracts whose mean distance is not statistically different from the minimal distance (Wilcoxon test; $p > 0.05$); and the green box plots represent tracts whose mean distance is statistically different from the minimal distance (Wilcoxon test; $p < 0.05$).

4.2.7. Semantic

As indicated by the cortical and subcortical distribution of semantic paraphasias (Fig. 3), semantic processing is supported by a large and distributed network, including the posterior and middle thirds of the STG and MTG, respectively, the DLPFC, and the IFG (Whitney et al., 2011). The subcortical distribution of semantic responses reflects the continuous and homogenous ventral course of functional information in the deep WM of the temporal lobe, from the occipital-temporal-parietal junction, through the ventral third of the external capsule, and ascending to the WM underneath the posterior two-thirds of IFG and MFG. This ventral workflow is crucial for the top-down control and contextualization of the semantic system (Duffau, 2015; Han et al., 2013). It is mainly subserved by IFOF, as confirmed in this series by the consistent overlap of subcortical and cortical semantic responses with the course of the IFOF (Fig. 5), from the posterior WM of the temporal lobe through the external capsule and up to its main territories of terminations within the frontal lobe (ventro-lateral and dorso-lateral cortices) (Sarubbo et al., 2015a, Sarubbo, 2016; Hau et al., 2016; Caverzasi et al., 2014). The IFOF is the

longest association bundle in the human brain, with the unique feature of terminating in the occipital, temporal, parietal, and frontal lobes (Hau et al., 2016; Caverzasi et al., 2014; Sarubbo et al., 2013; Martino et al., 2010). This long-range link between distant functional nodes was demonstrated to be crucial in mapping visual information into meaning, according to the classical role of the ventral stream (Duffau, 2015; Sarubbo et al., 2015a; 2008).

4.2.8. Non-verbal comprehension disorders

Non-verbal comprehension disorders identified with palm-pyramid-tree test (PPTT) were mainly located in the right hemisphere with a cortical distribution analogous to semantic paraphasias in the left hemisphere (Fig. 3). In fact, these responses are distributed across the parietal, temporal, and frontal regions with a prevalent ventral course matching the course of the IFOF, in particular at the level of the WM of the ventral third of the external capsule between the temporal and frontal lobes. These data support the hypothesis of a hemispheric segregation between verbal and non-verbal semantics (Moritz-Gasser et al., 2013;

Table 2

Overall distribution of the functional responses elicited at the cortical level according to a matching analysis with the JHU Atlas (cortical and cortical plus white matter ROIs). For each functional category, the percentage of DES-defined positive cortical sites that overlap with a given ROI is presented. For example, 32.4% of cortical sites where anomia was elicited with direct electrical stimulation overlapped with the JHU Atlas-defined left superior temporal gyrus, and 1.3% overlapped with the JHU Atlas-defined left superior temporal gyrus white matter. MFG: middle frontal gyrus; MTG: middle temporal gyrus; IFG: inferior frontal gyrus; ITG: inferior temporal gyrus; PreCG: pre-central gyrus; PostCG: post-central gyrus; SFG: superior frontal gyrus; SMG: supra marginal gyrus; SPL: superior parietal lobule; STG: superior temporal gyrus; WM: white matter.

	Left hemisphere	Right hemisphere
Alexia	MTG (90.3%), ITG (7.2%), MTG WM (2.4%)	–
Anomia	STG (32.4%), ITG (17.1%), MTG (17.1%), MFG (10.2%), SMG (4.7%), IFG WM (2.3%), STG WM (1.3%)	STG (2.4%)
Comprehension	MTG (20.3%), MFG (8.9%), STG (7%),	MFG (24.9%), IFG (16.5%), STG (6.3%), MTG (5.3%), MFG WM (2.3%), IFG WM (1.6%), SMG (1.3%)
Eye Movement Control	–	PreCG WM (65.9%), PreCG (27.1%), PostCG (7.1%)
Mentalizing	–	MFG (62.1%), IFG (22%), SFG (6.6%), MFG WM (6.5%), IFG WM (2.7%)
Motor	PreCG (18.2%), PostCG (8.3%), MFG (6.7%), PreCG WM (2.5%), SFG (1.9%), IFG (1.1%)	PreCG (22.7%), PostCG (12.3%), SFG (5.2%), MFG (4.9%), PreCG WM (4.1%), IFG (2.1%), STG (1.8%), PostCG WM (1.7%), SPL (1.2%)
Motor Control	MFG (9.9%), SFG (8.8%), PreCG (7%), PostCG (4.4%), SMG (2.3%), PostCG WM (1.7%), PreCG WM (1.5%), IFG (1%)	PreCG (26.4%), MFG (9.1%), STG (8.3%), SFG (4.1%), PreCG WM (4%), IFG (4%), PostCG (2.7%), STG WM (1.1%)
Phonological	SMG (31.4%), MFG (22.9%), MTG (21.4%), IFG (12.6%), SMG WM (3.6%), MFG WM (2.7%), STG (2%), ITG (1.5%)	–
Semantic	MFG (24.2%), STG (22.5%), IFG (21.6%), MTG (20.1%), IFG WM (3.2%), MFG WM (2.6%), STG WM (1.5%), PostCG (1%)	STG (1.5%)
Somatosensory	PostCG (26%), PreCG (5.3%), PostCG WM (4.6%), SMG (3.4%), SPL (1.4%)	PostCG (32%), PreCG (6.1%), SPL (5.6%), PostCG WM (5.4%), SMG (5.4%)
Spatial perception	SMG (5.9%)	SMG (40.9%), STG (25.1%), MTG (8.7%), SMG WM (5.9%), MFG (4.1%), STG WM (3.2%), SPL (1.8%), MFG WM (1.5%)
Speech Output	PreCG (27.3%), IFG (11.1%), PostCG (10.6%), PreCG WM (4.3%), SMG (4%), STG (4%), MTG (3.9%), IFG WM (1.8%)	PreCG (10.4%), IFG (5.2%), STG (5%), PostCG (3.1%), PreCG WM (2%), SMG (1.8%), MFG (1.8%), IFG WM (1%)
Speech Articulation	PostCG (19.9%), MFG (9.1%), PreCG (7.4%), IFG (7.2%), SMG (4.5%), STG (3.7%), PostCG WM (1.5%), IFG WM (1.3%)	PreCG (14.8%), IFG (11.2%), MFG (5.4%), PostCG (5.4%), PreCG WM (3.4%), STG (1.7%)

Han et al., 2013), with the latter mediated by the right IFOF (Herbet et al., 2017).

4.2.9. Phonologic

Phonological disturbances revealed a large and typical distribution over the cortices and subcortical WM connecting the ventral and mid-dorsal cortices of the posterior frontal lobe (particularly, IFG and MFG) with the posterior two-thirds of the temporal lobe (particularly, STG and MTG) (Fig. 3). We found a consistent match of the cortical and subcortical responses with the course and terminations of the AF. This multi-layer bundle (Sarubbo, 2016; Fernandez-Miranda et al., 2015) is the main component of the dorsal pathways and constitutes the essential structural core for long-range connection among the phonological epicenters that are largely distributed around the peri-sylvian cortices (Thiebaut de Schotten et al., 2011a; Duffau et al., 2014; Corina et al., 2010; Maldonado et al., 2011). The parallel course of the two main components of dorsal stream, AF (medially) and indirect anterior SLF (also known as SLF III, laterally) that connects the ventral frontal lobe with the inferior parietal lobule (IPL) (Sarubbo, 2016; Catani et al., 2005; Martino et al., 2013), reflects the parallel and segregated distribution of, respectively, subcortical phonological and verbal apraxia responses. The adjacent and partially overlapping territories of termination of these bundles in the frontal lobe and IPL also reflects the distribution of the phonological and verbal apraxia responses at the cortical level, as in previous reports (Sarubbo, 2016; Vigneau et al., 2006). This intricate functional anatomy constitutes the essential background for the strict integration of the dorsal route. Our data suggest that in this system, auditory and somato-sensory speech inputs are transferred via direct AF fibers from the posterior two thirds of STG/MTG to the IFG (particularly, pars opercularis and triangularis), to be converted in working phonological–phonetic representations. This information is then translated into articulatory motor outputs mediated by the VPMC, which receives feedback information from somatosensory and auditory areas at the junction between STG and SMG and the ventral PostCG, via the SLF III (Duffau, 2015; Duffau et al., 2014).

4.2.10. Visual and reading

The distribution of visual deficits (Fig. 4) reflects the classical distribution of visual pathways underlying the temporal-occipital regions, including the primary visual area and optic radiations (Sarubbo et al., 2015b).

Reading deficits were mainly distributed in the left MTG and inferior temporal gyrus (ITG), and in the basolateral WM of ITG and fusiform gyrus (Fig. 4), corresponding to the course of the dorsal portion of ILF (Sarubbo, 2016). These cortical territories are also known as the visual word form area (VWFA) and are structurally involved in the elaboration of visual information, integrating inputs coming from the ipsilateral and contralateral occipital pole, via the posterior-dorsal portion of ILF and CC, respectively (Zemmoura et al., 2015; Herbert et al., 2018). The ILF is a double component long bundle connecting the dorso-lateral and ventral cortices of the occipital lobe to the antero-lateral and anterior and basal temporal cortices (Sarubbo, 2016; De Benedictis et al., 2014; Catani et al., 2003; Mandonnet et al., 2009). This pathway is the main WM tract implicated in both the direct and indirect transfer of information between the occipital visual territories and temporal limbic and memory areas. The ILF subserves several aspects of visual input processing, such as face recognition, reading, visual perception and memory (Mandonnet et al., 2009). Finally, this occipital-temporal system is bi-directionally modulated by connections with the IPL, via the indirect posterior portion of the SLF, connecting the posterior third of STG and MTG with the AG and the SMG, and providing an interactive feedback between visual and non-visual information (Zemmoura et al., 2015; Dehaene et al., 2005).

4.2.11. Spatial perception

Spatial perception error responses are strongly right-lateralized, as previously reported (Thiebaut de Schotten et al., 2011b, 2012) and are distributed over the cortices of SMG, posterior portion of STG and within the WM crossing the IPL and the superior-posterior portion of the temporal lobe (Fig. 4). This largely integrated cortico-subcortical network subserves the symmetrical processing of visual scene, attention, and awareness. For this reason, several different qualitative and quantitative

Table 3

Distribution of the functional responses elicited in the white matter according to the matching analysis with the ROIs of JHU Atlas (cortical and cortical plus white matter ROIs). For each functional category, the percentage of DES-defined subcortical white matter positive sites that overlap with a given ROI is presented. For example, 28.4% of sites where alexia was elicited with direct electrical stimulation of the subcortical white matter during Reading task overlapped with the JHU Atlas-defined left inferior temporal gyrus, and 5.8% overlapped with the JHU Atlas-defined left inferior temporal gyrus white matter. AG: angular gyrus; CG: cingulate gyrus; FG: fusiform gyrus; FOC: fronto-orbital cortex; MFG: middle frontal gyrus; MOG: middle occipital gyrus; MTG: middle temporal gyrus; IFG: inferior frontal gyrus; IOG: inferior occipital gyrus; ITG: inferior temporal gyrus; PreCG: pre-central gyrus; PostCG: post-central gyrus; SFG: superior frontal gyrus; SMG: supra marginal gyrus; SOG: superior occipital gyrus; SPL: superior parietal lobule; STG: superior temporal gyrus; WM: white matter.

	Left hemisphere	Right hemisphere
Acoustic responses	STG (31%), STG WM (21.1%), MTG (2.9%)	STG (20.4%), MTG (14.1%), STG WM (5.5%), MTG WM (4.9%)
Reading	ITG (28.4%), FG (21.5%), MTG (8.2%), IOG (6.5%), ITG WM (5.8%), MTG WM (5.3%), FG WM (5.2%), IOG WM (3.4%)	ITG (4.3%), ITG WM (2.4%)
Anomia	STG (11.5%), MFG (8.1%), MFG WM (7.8%), AG (7.4%), AG WM (7%), MTG (6.9%), ITG (6.6%), STG WM (4.1%), IFG WM (3.3%), SMG (2.9%), insula (2.6%), lateral FOC (2.5%), ITG WM (2.3%), MTG WM (2%), IFG (1.9%), SMG WM (1.3%), lateral FOC WM (1.1%), FG (1%)	AG WM (3.8%), AG (1.8%), MTG WM (1%)
Comprehension	SPL (3.3%), STG (3.2%), insula (2.9%), SPL WM (2.6%), SMG WM (2.1%), MFG WM (1.7%), STG WM (1.2%)	MFG WM (9.7%), STG (7%), hippocampus (6.9%), MFG (6.7%), STG WM (6.6%), AG WM (6.6%), MTG WM (4.9%), AG (3.9%), insula (3.6%), ITG WM (2.7%), ITG (2%), PostCG (1.2%), SMFG (1.2%), MTG (1.1%)
Eye movement Control	MFG (23.4%), MFG WM (19.3%), SFG WM (4%), PreCG (3.8%), PreCG WM (3.6%), SFG (2.2%)	MFG (19.6%), MFG WM (9.5%), SFG (3.8%), SFG WM (1.3%)
Language and Motor Planning	CN (13.9%), SFG WM (6%), SFG (4.9%), MFG WM (3%), insula (2.9%), IFG (2.4%), lateral FOC WM (2.1%), IFG WM (1.9%), MFG (1.8%), Putamen (1.4%), lateral FOC (1.1%)	CN (1.3%)
Mentalizing	–	MFG WM (12.4%), IFG (9.9%), MFG (9.2%), SFG (8.8%), IFG WM (6.7%), SFG WM (6.5%), CG (3.7%), CN (3.3%), insula (1%)
Motor	PreCG WM (5.2%), SFG (4.6%), PreCG (4.5%), SFG WM (4.2%), putamen (2.4%), insula (2.3%), MFG (1.7%)	preCG WM (5.9%), SFG (5.2%), putamen (4.9%), SFG WM (4.6%), PreCG (4.3%), insula (4.2%), MFG (3.3%), MFG WM (2.4%), PostCG (2.1%), SLF (2.1%), PostCG WM (1.6%), IFG (1.2%), IFG WM (1%)
Motor Control	SFG WM (8.9%), SFG (7.5%), MFG WM (3.4%), MFG (3.1%), CG (1.7%), PostCG WM (1.4%), PostCG (1.3%), preCG (1.1%)	SFG (10.3%), SFG WM (6.9%), MFG (4.9%), CG (4.7%), IFG (4.6%), IFG WM (4.2%), insula (2.8%), MFG WM (2.5%), putamen (1.9%), precuneus (1.4%)
Phonological	ITG (10.3%), MTG (8.4%), MTG WM (7.9%), FG (6.3%), IFG WM (5.8%), STG (4.9%), SPL WM (3.6%), ITG WM (3.2%), IFG (2.9%), MFG (2.8%), STG WM (2.7%), AG WM (2.4%), MFG WM (2.4%), PostCG WM (2%), SS (2%), PreCG WM (1.9%), AG (1.9%), PostCG (1.9%), SPL (1.8%), SMG WM (1.5%), PreCG (1.5%), SMG (1.4%), insula (1.2%)	–
Semantic	MTG WM (7.7%), insula (6.9%), MTG (5.7%), STG (5.5%), hippocampus (4.9%), MFG WM (4.6%), ITG (4.6%), ITG (4.6%), FG (4.4%), ITG WM (4.6%), STG WM (3.9%), MFG 3.2%), IFG (3.1%), IFG WM (2.7%), putamen (2%), lateral FOC (2%), FG WM (1.7%), SFG WM (1.3%)	–
Somatosensory	SPL WM (6.2%), SPL (2.9%), PostCG WM (2.7%), precuneus (2.5%), PostCG (1.2%), preCG (1.2%), PreCG WM (1.1%)	SPL (8.6%), PostCG WM (8.3%), PostCG (8.1%), SPL WM (7.1%), SMG (6.7%), AG (4.6%), SMG (4.6%), insula (3%), pre-cuneus (2.4%), STG (2.2%), AG WM (2%), PreCG (1.7%)
Spatial perception	AG WM (6.7%), AG (6.2%)	SMG (17.1%), SMG WM (11.9%), AG (10.5%), AG WM (6.7%), STG (4.4%), SPL WM (4.2%), STG WM (3.3%), MFG WM (3.2%), PostCG WM (2.6%), SPL (1.9%), CG (1.6%), MTG (1.5%), PreCG WM (1.3%), MFG (1.3%)
Speech Output	IFG (11.4%), IFG WM (10.7%), PreCG (8%), PreCG WM (7.7%), MFG (5.2%), STG (5.1%), insula (4.1%), MFG WM (2.5%), STG WM (1.7%)	PreCG WM (6.1%), PreCG (6%), MFG (4.1%), IFG (3.8%), insula (3.6%), MFG WM (3.3%), IFG WM (3.1%), putamen (1.6%)
Speech Articulation	SMG WM (10.6%), SMG (10.5%), PostCG (6.1%), PreCG WM (6.1%), PostCG WM (5.2%), PreCG (5.1%), IFG (4.1%), MFG (4%), IFG WM (3.6%), MFG WM (3.2%), STG (3.1%), AG WM (2.9%), AG (2.8%), insula (2.5%), SFG WM (1.2%)	SMG (2.6%), SMG WM (2.4%), IFG (2.3%), MFG (2.2%), SFG WM (1.6%), MFG WM (1.3%)
Visual	FG (8.6%), IOG WM (3.1%), FG WM (2.9%), MOG WM (1.9%), IOG (1.5%)	AG WM (9%), AG (5.4%), IOG (4.1%), MTG WM (3.8%), MOG WM (3.3%), Hippocampus (3.1%), FG (2.7%), IOG WM (2.3%), SPL WM (2%), SOG WM (1.8%), MOG (1.6%), MTG (1.5%), ITG (1.5%), FG WM (1.2%), STG WM (1%), SMG WM (1%)

clinical manifestations have been described, depending on different patterns of cortical damage and WM disconnection (2012; Doricchi et al., 2008; Verdon et al., 2010). The distribution of cortical and subcortical responses in this atlas confirmed that SMG and the posterior-superior STG are the main cortical hubs. Accordingly, the WM underlying the IPL, especially at the level of SMG where dorsal and ventral components of SLF (i.e. II and III, respectively) have parallel course and adjacent terminations (Thiebaut de Schotten et al., 2011a; Makris et al., 2005; Vallar et al., 2013; Wang et al., 2016), is the essential anatomical substrate for spatial awareness (Sarubbo et al., 2015a; 2011b). Finally, the subcortical responses elicited in the mid-dorsal WM of the frontal lobe, along the anterior course of SLF, highlight the basic fronto-parietal functional integration subserved by these fibers (Lunven et al., 2015).

4.2.12. Mentalizing

Mentalizing is a socio-cognitive process that enables humans to

understand, and consequently predict, mental and psychological states (intentions or emotions) and behaviors of others. Previous studies demonstrated that mentalizing abilities are subserved by neural sub-systems, namely the mirror neural network and the mentalizing network coding, respectively, for low-level perceptive socio-cognitive processes and high-level reflective processing (Amodio and Frith, 2006; Molnar-Szakacs and Uddin, 2013). In a previous work, the application of specific intraoperative behavioral tasks during DES mapping allowed to differentiate two functional sub-systems, respectively at the posterior infero-lateral prefrontal regions (low-level perceptual) and at the dorso-mesial prefrontal territory (high-level inferential) (Herbet et al., 2014). The whole distribution of functional epicenters for mentalizing in the same portion of IFG and SFG (Fig. 4) and in the WM of the frontal lobe connecting these ventral and dorsal cortices, confirms a crucial role of mid-posterior frontal lobe in different aspects of emotional and social cognitive intelligence (Yordanova et al., 2017).

4.2.13. Acoustic

Acoustic responses were classically located along the posterior third of the *planum temporalis* and the WM underneath, connecting the auditory cortex of the Heschl's gyrus with the medial geniculate nucleus of the thalamus (Fig. 4). Although no tractography atlas reconstructing the acoustic radiations are available, the subcortical distribution of these functional responses matches the course of the acoustic radiations, as recently renewed by high-resolution tractography and micro-dissection (Maffei et al., 2018).

4.3. Limitations

Our dataset, although unique given the different aspects highlighted above, does have some limitations. First, we propose data coming from a pathological model which assumes limited plasticity despite tumor involvement. Although tumor-induced plasticity may occur, LGGs have been shown to represent a valid model for exploring normal brain functions, and in fact, DES has been consistently utilized to confirm previous hypotheses of human brain processing (Duffau, 2015). As discussed above, the overall distribution of the functional responses is topographically congruent with the atlases used for matching analyses and the current literature, including large meta-analysis involving healthy human subjects. Finally, the large number of responses in this study (1821 responses in 256 patients) of patients with widely distributed tumor locations should minimize the contribution of plasticity effects in individual patients to our overall statistically-derived functional maps.

A second limitation relates to the collection of only positive functional responses in our series, in spite of a homogenous distribution of these responses over the brain at both cortical and subcortical levels. To minimize this possible issue, we adopted a solid multinomial statistical analysis and provided the confidence intervals plots of the positive critical nodes across our large functional datasets for both number of stimulations and subjects tested. The exploration with DES of the entire exposed cortex and subcortical WM in each mapping session, including beyond the margins of the tumor, contributed to provide reliability to this data set.

Third, we utilized a linear transformation methods for normalizing patients brains to the MNI-125 atlas. While this may introduce some degree of error during normalization, we found that the linear approach worked best in our dataset, due to a combination of factors including brain shift, local mass effect, resection cavity distortion, and ventricular changes. The consistent matching of our data with prior independently published cortical/subcortical atlases (which was a second check of reliability) confirms that our registration approach was reasonable and accurate.

Lastly, given time limitations of surgery we were unable to test all 16 functional domains at each cortical and subcortical point, which may have biased our mapping of some functions to certain anatomic locations.

5. Conclusions

We computed the first integrated cortical-subcortical multi-functional probabilistic map of human brain processing, as emerged from direct electrical mapping during clinical and neuropsychological testing. The data discussed are concordant with the current literature and different multi-modal studies, and also provide new insights into the structural and functional organization of different networks. Finally, the unprecedented volume of functional responses collected, the large number of patients included, and the unique value of the WM distribution of the functional responses reported, allow for a reliable and complementary tool for multi-modal analyses exploring the structure and function of brain processing in humans.

Ethics statement

The present study has been carried out in accordance with The Code

of Ethics of the World Medical Association (Declaration of Helsinki) for experiments involving humans and was approved by the local Institutional Review Board.

Funding

Research reported in this publication was supported, in part, by the National Institutes of Health's National Center for Advancing Translational Sciences, Grant Number KL2TR001424 (MT). The content is solely the responsibility of the authors and does not necessarily represent the official views of the National Institutes of Health.

Declaration of competing interest

No authors have disclosures or conflict of interest regarding this work.

References

- Alexander, G.E., Crutcher, M.D., 1990. Functional architecture of basal ganglia circuits: neural substrates of parallel processing. *Trends Neurosci.* 13, 266–271.
- Amodio, D.M., Frith, C.D., 2006. Meeting of minds: the medial frontal cortex and social cognition. *Nat. Rev. Neurosci.* <https://doi.org/10.1038/nrn1884>.
- Bartolomeo, P., De Schotten, M.T., Duffau, H., 2007. Mapping of visuospatial functions during brain surgery: a new tool to prevent unilateral spatial neglect [5]. *Neurosurgery*. <https://doi.org/10.1227/01.neu.0000306126.46657.79>.
- Catani, M., Jones, D.K., Donato, R., Ffytche, D.H., 2003. Occipito-temporal connections in the human brain. *Brain* 126, 2093–2107.
- Catani, M., Jones, D.K., Ffytche, D.H., 2005. Perisylvian language networks of the human brain. *Ann. Neurol.* 57, 8–16.
- Catani, M., et al., 2012. Short frontal lobe connections of the human brain. *Cortex* 48, 273–291.
- Caverzasi, E., Papinutto, N., Amirbekian, B., Berger, M.S., Henry, R.G., 2014. Q-ball of inferior fronto-occipital fasciculus and beyond. *PLoS One* 9.
- Coello, A.F., et al., 2013. Selection of intraoperative tasks for awake mapping based on relationships between tumor location and functional networks. *J. Neurosurg.* <https://doi.org/10.3171/2013.6.JNS122470>.
- Corina, D.P., et al., 2010. Analysis of naming errors during cortical stimulation mapping: implications for models of language representation. *Brain Lang.* <https://doi.org/10.1016/j.bandl.2010.04.001>.
- Courtney, S.M., Petit, L., Maisog, J.M., Ungerleider, L.G., Haxby, J.V., 1998. An area specialized for spatial working memory in human frontal cortex. *Science* 279, 1347–1351, 80.
- Crivellato, E., Ribatti, D., 2007. Soul, mind, brain: Greek philosophy and the birth of neuroscience. *Brain Res. Bull.* 71, 327–336.
- De Benedictis, A., et al., 2014. Anatomic-functional study of the temporo-parieto-occipital region: dissection, tractographic and brain mapping evidence from a neurosurgical perspective. *J. Anat.* 225.
- Dehaene, S., Cohen, L., Sigman, M., Vinckier, F., 2005. The neural code for written words: a proposal. *Trends Cogn. Sci.* <https://doi.org/10.1016/j.tics.2005.05.004>.
- Deloche, G., et al., 1991. The effects of age, educational background and sex on confrontation naming in normals; principles for testing naming ability. *Aphasiology*. <https://doi.org/10.1080/02687039108248566>.
- Doricchi, F., Thiebaut de Schotten, M., Tomaiuolo, F., Bartolomeo, P., 2008. White matter (dis)connections and gray matter (dys)functions in visual neglect: gaining insights into the brain networks of spatial awareness. *Cortex* 44, 983–995.
- Duffau, H., 2015. Stimulation mapping of white matter tracts to study brain functional connectivity. *Nat. Rev. Neurol.* 11, 255–265.
- Duffau, H., et al., 2003. Usefulness of intraoperative electrical subcortical mapping during surgery for low-grade gliomas located within eloquent brain regions: functional results in a consecutive series of 103 patients. *J. Neurosurg.* 98, 764–778.
- Duffau, H., et al., 2005. Contribution of intraoperative electrical stimulations in surgery of low grade gliomas: a comparative study between two series without (1985–96) and with (1996–2003) functional mapping in the same institution. *J. Neurol. Neurosurg. Psychiatry* 76, 845–851.
- Duffau, H., et al., 2005. New insights into the anatomic-functional connectivity of the semantic system: a study using cortico-subcortical electrostimulations. *Brain* 128, 797–810.
- Duffau, H., Leroy, M., Gatignol, P., 2008. Cortico-subcortical organization of language networks in the right hemisphere: an electrostimulation study in left-handers. *Neuropsychologia* 46, 3197–3209.
- Duffau, H., Moritz-Gasser, S., Mandonnet, E., 2014. A re-examination of neural basis of language processing: proposal of a dynamic hodotopical model from data provided by brain stimulation mapping during picture naming. *Brain Lang.* 131, 1–10.
- Evans, A.C., et al., 1992. Anatomical mapping of functional activation in stereotactic coordinate space. *Neuroimage* 1, 43–53.
- Fernandez-Miranda, J.C., et al., 2015. Asymmetry, connectivity, and segmentation of the arcuate fascicle in the human brain. *Brain Struct. Funct.* 220, 1665–1680.
- Fox, M.D., 2018. Mapping symptoms to brain networks with the human connectome. *N. Engl. J. Med.* 379, 2237–2245.

- Gras-Combe, G., Moritz-Gasser, S., Herbet, G., Duffau, H., 2012. Intraoperative subcortical electrical mapping of optic radiations in awake surgery for glioma involving visual pathways. *J. Neurosurg.* 117, 466–473.
- Han, Z., et al., 2013. White matter structural connectivity underlying semantic processing: evidence from brain damaged patients. *Brain* 136, 2952–2965.
- Hau, J., et al., 2016. Cortical terminations of the inferior fronto-occipital and uncinate fasciculi: stem-based anatomical virtual dissection. *Front. Neuroanat.* 10, 58.
- Hau, J., et al., 2017. Revisiting the human uncinate fasciculus, its subcomponents and asymmetries with stem-based tractography and microdissection validation. *Brain Struct. Funct.* 222, 1645–1662.
- Herbet, G., et al., 2014. Inferring a dual-stream model of mentalizing from associative white matter fibres disconnection. *Brain* 137, 944–959.
- Herbet, G., Lafargue, G., Moritz-Gasser, S., Bonnetblanc, F., Duffau, H., 2015. Interfering with the neural activity of mirror-related frontal areas impairs mentalistic inferences. *Brain Struct. Funct.* <https://doi.org/10.1007/s00429-014-0777-x>.
- Herbet, G., et al., 2016. Converging evidence for a cortico-subcortical network mediating lexical retrieval. *Brain* 139, 3007–3021.
- Herbet, G., Moritz-Gasser, S., Duffau, H., 2017. Direct evidence for the contributive role of the right inferior fronto-occipital fasciculus in non-verbal semantic cognition. *Brain Struct. Funct.* 222, 1597–1610.
- Herbet, G., Zemmoura, I., Duffau, H., 2018. Functional anatomy of the inferior longitudinal fasciculus: from historical reports to current hypotheses. *Front. Neuroanat.* <https://doi.org/10.3389/fnana.2018.00077>.
- Hoffstaedter, F., Grefkes, C., Zilles, K., Eickhoff, S.B., 2012. The ‘what’ and ‘when’ of self-initiated movements. *Cerebr. Cortex.* <https://doi.org/10.1093/cercor/bhr391>.
- Hutchison, R.M., et al., 2013. Dynamic functional connectivity: promise, issues, and interpretations. *Neuroimage* 80, 360–378.
- Ius, T., Angelini, E., Thiebaut de Schotten, M., Mandonnet, E., Duffau, H., 2011. Evidence for potentials and limitations of brain plasticity using an atlas of functional resectability of WHO grade II gliomas: towards a “minimal common brain”. *Neuroimage* 56, 992–1000.
- Lunven, M., et al., 2015. White matter lesion predictors of chronic visual neglect: a longitudinal study. *Brain* 138, 746–760.
- Maffei, C., et al., 2018. Topography of the human acoustic radiation as revealed by ex vivo fibres micro-dissection and in vivo diffusion-based tractography. *Brain Struct. Funct.* 223.
- Maier-Hein, K.H., et al., 2017. The challenge of mapping the human connectome based on diffusion tractography. *Nat. Commun.* 8.
- Makris, N., et al., 2005. Segmentation of subcomponents within the superior longitudinal fascicle in humans: a quantitative, in vivo, DT-MRI study. *Cerebr. Cortex* 15, 854–869.
- Maldonado, I.L., et al., 2011. Surgery for gliomas involving the left inferior parietal lobule: new insights into the functional anatomy provided by stimulation mapping in awake patients. *J. Neurosurg.* <https://doi.org/10.3171/2011.5.JNS112>.
- Mandonnet, E., Gatignol, P., Duffau, H., 2009. Evidence for an occipito-temporal tract underlying visual recognition in picture naming. *Clin. Neurol. Neurosurg.* 111, 601–605.
- Mandonnet, E., Sarubbo, S., Duffau, H., 2017. Proposal of an optimized strategy for intraoperative testing of speech and language during awake mapping. *Neurosurg. Rev.* 40, 29–35.
- Martino, J., Brogna, C., Robles, S.G., Vergani, F., Duffau, H., 2010. Anatomic dissection of the inferior fronto-occipital fasciculus revisited in the lights of brain stimulation data. *Cortex* 46, 691–699.
- Martino, J., et al., 2013. Analysis of the subcomponents and cortical terminations of the perisylvian superior longitudinal fasciculus: a fiber dissection and DTI tractography study. *Brain Struct. Funct.* 218, 105–121.
- Matsumoto, R., et al., 2004. Functional connectivity in the human language system: a cortico-cortical evoked potential study. *Brain.* <https://doi.org/10.1093/brain/awh246>.
- Matsumoto, R., et al., 2012. Parieto-frontal network in humans studied by cortico-cortical evoked potential. *Hum. Brain Mapp.* 33, 2856–2872. <https://doi.org/10.1002/hbm.21407>.
- Michel, C.M., Murray, M.M., 2012. Towards the utilization of EEG as a brain imaging tool. *NeuroImage.* <https://doi.org/10.1016/j.neuroimage.2011.12.039>.
- Molnar-Szakacs, I., Uddin, L.Q., 2013. Self-processing and the default mode network: interactions with the mirror neuron system. *Front. Hum. Neurosci.* <https://doi.org/10.3389/fnhum.2013.00571>.
- Montemurro, N., Herbet, G., Duffau, H., 2016. Right cortical and axonal structures eliciting ocular deviation during electrical stimulation mapping in awake patients. *Brain Topogr.* <https://doi.org/10.1007/s10548-016-0490-6>.
- Moritz-Gasser, S., Herbet, G., Duffau, H., 2013. Mapping the connectivity underlying multimodal (verbal and non-verbal) semantic processing: a brain electrostimulation study. *Neuropsychologia* 51, 1814–1822.
- Penfield, W., Boldrey, E., 1937. Somatic motor and sensory representation in the cerebral cortex of man as studied by electrical stimulation. *Brain* 60, 389–443.
- Petersen, S.E., Sporns, O., 2015. Brain networks and cognitive architectures. *Neuron* 88, 207–219.
- Pujol, S., et al., 2015. The DTI challenge: toward standardized evaluation of diffusion tensor imaging tractography for neurosurgery. *J. Neuroimaging* 25, 875–882.
- Rech, F., Herbet, G., Moritz-Gasser, S., Duffau, H., 2014. Disruption of bimanual movement by unilateral subcortical electrostimulation. *Hum. Brain Mapp.* 35, 3439–3445.
- Rech, F., Herbet, G., Moritz-Gasser, S., Duffau, H., 2016. Somatotopic organization of the white matter tracts underpinning motor control in humans: an electrical stimulation study. *Brain Struct. Funct.* 221, 3743–3753.
- Sanai, N., Berger, M.S., 2010. Intraoperative stimulation techniques for functional pathway preservation and glioma resection. *Neurosurg. Focus* 28, E1.
- Sanai, N., Mirzadeh, Z., Berger, M.S., 2008. Functional outcome after language mapping for glioma resection. *N. Engl. J. Med.* 358, 18–27.
- Sarubbo, S., et al., 2016. Structural and functional integration between dorsal and ventral language streams as revealed by blunt dissection and direct electrical stimulation. *Hum. Brain Mapp.* 37, 3858–3872.
- Sarubbo, S., De Benedictis, A., Maldonado, I.L., Basso, G., Duffau, H., 2013. Frontal terminations for the inferior fronto-occipital fascicle: anatomical dissection, DTI study and functional considerations on a multi-component bundle. *Brain Struct. Funct.* 218.
- Sarubbo, S., et al., 2015. Towards a functional atlas of human white matter. *Hum. Brain Mapp.* 36, 3117–3136.
- Sarubbo, S., et al., 2015. The course and the anatomo-functional relationships of the optic radiation: a combined study with ‘post mortem’ dissections and ‘in vivo’ direct electrical mapping. *J. Anat.* 226, 47–59.
- Schucht, P., Moritz-Gasser, S., Herbet, G., Raabe, A., Duffau, H., 2013. Subcortical electrostimulation to identify network subserving motor control. *Hum. Brain Mapp.* 34, 3023–3030.
- Sporns, O., 2013. The human connectome: origins and challenges. *Neuroimage* 80, 53–61.
- Tate, M.C., Herbet, G., Moritz-Gasser, S., Tate, J.E., Duffau, H., 2014. Probabilistic map of critical functional regions of the human cerebral cortex: Broca’s area revisited. *Brain* 137, 2773–2782.
- Thiebaut de Schotten, M., et al., 2005. Direct evidence for a parietal-frontal pathway subserving spatial awareness in humans. *Science* 309, 2226–2228.
- Thiebaut de Schotten, M., et al., 2011. Atlasing location, asymmetry and inter-subject variability of white matter tracts in the human brain with MR diffusion tractography. *Neuroimage* 54, 49–59.
- Thiebaut de Schotten, M., et al., 2011. A lateralized brain network for visuospatial attention. *Nat. Neurosci.* 14, 1245–1246.
- Thiebaut de Schotten, M., et al., 2012. Damage to white matter pathways in subacute and chronic spatial neglect: a group study and 2 single-case studies with complete virtual ‘in vivo’ tractography dissection. *Cerebr. Cortex.* <https://doi.org/10.1093/cercor/bhs351>.
- Toga, A.W., Thompson, P.M., Mori, S., Amunts, K., Zilles, K., 2006. Towards multimodal atlases of the human brain. *Nat. Rev. Neurosci.* <https://doi.org/10.1038/nrn2012>.
- Vallar, G., et al., 2013. Cerebral correlates of visuospatial neglect: a direct cerebral stimulation study. *Hum. Brain Mapp.* <https://doi.org/10.1002/hbm.22257>.
- van den Heuvel, M.P., et al., 2017. Proportional thresholding in resting-state fMRI functional connectivity networks and consequences for patient-control connectome studies: issues and recommendations. *Neuroimage* 152, 437–449.
- Verdon, V., Schwartz, S., Lovblad, K.-O., Hauert, C.-A., Vuilleumier, P., 2010. Neuroanatomy of hemispatial neglect and its functional components: a study using voxel-based lesion-symptom mapping. *Brain* 133, 880–894.
- Vigneau, M., et al., 2006. Meta-analyzing left hemisphere language areas: phonology, semantics, and sentence processing. *NeuroImage* 30, 1414–1432.
- Wang, X., et al., 2016. Subcomponents and connectivity of the superior longitudinal fasciculus in the human brain. *Brain Struct. Funct.* 221, 2075–2092.
- Whitney, C., Kirk, M., O’Sullivan, J., Lambon Ralph, M.A., Jefferies, E., 2011. The neural organization of semantic control: TMS evidence for a distributed network in left inferior frontal and posterior middle temporal gyrus. *Cerebr. Cortex.* <https://doi.org/10.1093/cercor/bhq180>.
- Wolpe, N., et al., 2014. The medial frontal-prefrontal network for altered awareness and control of action in corticobasal syndrome. *Brain.* <https://doi.org/10.1093/brain/awt302>.
- Yordanova, Y.N., Duffau, H., Herbet, G., 2017. Neural pathways subserving face-based mentalizing. *Brain Struct. Funct.* <https://doi.org/10.1007/s00429-017-1388-0>.
- Zacà, D., et al., 2018. Whole-brain network connectivity underlying the human speech articulation as emerged integrating direct electric stimulation, resting state fMRI and tractography. *Front. Hum. Neurosci.* <https://doi.org/10.3389/fnhum.2018.00405>.
- Zemmoura, I., Herbet, G., Moritz-Gasser, S., Duffau, H., 2015. New insights into the neural network mediating reading processes provided by cortico-subcortical electrical mapping. *Hum. Brain Mapp.* <https://doi.org/10.1002/hbm.22766>.
- Zhang, Y., et al., 2010. Atlas-guided tract reconstruction for automated and comprehensive examination of the white matter anatomy. *Neuroimage* 52, 1289–1301.